Variable Voltage Control of a Hybrid Energy Storage System for Firm Frequency Response in the UK

Jianwei Li, Fang Yao, Qingqing Yang, Zhongbao Wei, and Hongwen He

Original citation & hyperlink:
Li, J., Yao, F., Yang, Q., Wei, Z. and He, H., 2022. Variable Voltage Control of a Hybrid Energy Storage System for Firm Frequency Response in the UK. *IEEE Transactions on Industrial Electronics*. (In Press)
https://dx.doi.org/10.1109/TIE.2022.3144590

DOI 10.1109/TIE.2022.3144590
ISSN 0278-0046
ESSN 1557-9948

Publisher: IEEE

This article has been accepted for publication in a future issue of this journal, but has not been fully edited. Content may change prior to final publication. Citation information: DOI 10.1109/TIE.2022.3144590, IEEE Transactions on Industrial Electronics

Variable Voltage Control of a Hybrid Energy Storage System for Firm Frequency Response in the UK

Jianwei Li, *Member, IEEE*, Fang Yao, Qingqing Yang, *Member, IEEE*, Zhongbao Wei, *Member, IEEE*, Hongwen He, *Senior Member, IEEE*

***Abstract*—**The National Grid in the UK, proposed the Firm Frequency Response (FFR) documents on recent developments regarding tendering options for active balancing mechanism units, specifically for batteries. However, frequent bipolar converting and instantaneous high power demand challenge battery lifetime and operation cost in the FFR. Combining a battery with a supercapacitor (SC) has several advantages, but the system cost may rise. Targeting at the FFR service, this paper presents a new variable voltage control within a semi-active battery-supercapacitor hybrid scheme. In proposed hybrid energy storage system (HESS), the DC bus voltage is controllable so that to improve the SC use ratio meanwhile reduce converters cost. A power management strategy integrating fuzzy logic with dynamic filtering method is proposed benefiting in broadening the filtering flexibility while reducing battery degradation. In addition, both the long-term simulations and scaled-down experiments are implemented to verify the proposed topology with the control strategy and power management by quantitative comparisons of battery degradations and SC use ratios.

Index Terms—Battery, hybrid energy storage system, firm frequency response, variable voltage control, supercapacitor

I. Introduction

Frequency Response (FR) is a necessary part of the power system, which is critical for the secure and stable operation of the grid [1, 2]. However, the large penetration of renewable energy sources (RES) into the grid brings a new challenge to grid frequency modulation [3]. Since the uncertainty of renewable energy sources, it cannot provide the inertial response like traditional generators [4]. Therefore, it is necessary to import a new frequency response mechanism. In the UK, National Grid Electricity Transmission, the primary energy transmission network operator, has introduced a new and fast service called Firm Frequency Response (FFR) specifically aimed at energy storage systems (ESSs), which could provide a real-time response to deviations in the grid frequency [5]. The FFR is the principle, based on which, the frequency regulation players (energy storage provider) calculate the power requirement for the energy storage system, and then sell the energy storage charge/discharge service to the Grid [6]. Basically, the FFR is the rule that energy storage providers used for determining how much charge/discharge service they may provide to the grid.

In recent years, the value of ESSs to provide fast frequency service has been more and more recognized [7]. Many recently published works introduce the application of battery energy storage systems in frequency regulation for both the distributed microgrid [8] as well as the large power system [9], regarding the control [10], sizing study [11], cost-effective analysis [12], etc. Aiming at the UK power system, Burcu et al [13] introduced the battery energy storage system for FFR, which is verified to be effective by the 1 MW/1 MWh lithium-titanate battery energy storage system (BESS) at the University of Sheffield. However, in terms of the power requirement for the frequency modulation, the battery system needs to respond to frequent bipolar power converting and sometimes, the instantaneous high-power demand [14]. Li et al [15] use the battery as the key element for the frequency control of an off-grid power system in an island. In this work, the fast and high-frequency power response causes extra damage to the battery's health. Swierczynski et al [16] investigated Li-ion BESS application in primary frequency regulation service and concluded that frequent charge/discharge will dramatically reduce battery service lifetime.

In order to extend battery life and achieve better frequency regulation performance, the idea of the hybrid energy storage system (HESS) has been proposed by many researchers [17-19]. The most general hybrid scheme employing supercapacitor-battery scheme has been investigated in different scenarios set to achieve various functions in the grid applications: supplying grid connected photovoltaic system with fast response [20]; maintaining voltage stability in both the AC system [21] and DC system [22, 23]; relieving the instantaneous power changes in the domestic CHP systems [24] and fast frequency control in both the large power system [25] and microgrid [26] with battery lifetime saving. HESS configurations can be classified in three main categories: passive, semi-active, and fully-active. Due to its high flexibility, modularity, and controllability, the fully-active topology has attracted more attention [27]. Although this topology could achieve optimal power allocation results, the construction cost of the DC/DC converters is higher as two DC/DC converters are needed [28]. The passive topology need no converter, however, the energy storage systems respond to power demand passively [29].

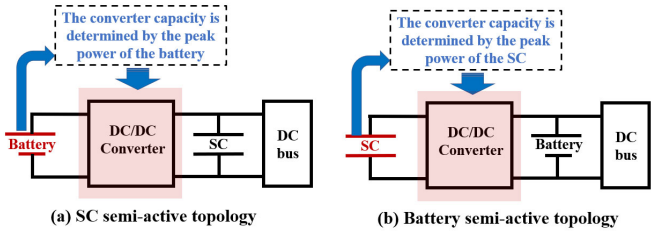

Fig. 1 The two semi-active topology

Semi-active topology could be divided into two different topologies: the battery semi-active topology as shown in Fig. 1(b) and the SC semi-active topology in Fig. 1(a) [28]. In battery

Jianwei Li, Fang Yao, Zhongbao Wei and Hongwen He are with Beijing Institute of Technology, Beijing 100081, China. Qingqing Yang is with Coventry Unversity, Coventry, CV1 5FB, UK.
Corresponding author: Qingqing Yang, E-mail: qingqing.yang@bath.edu.

This article has been accepted for publication in a future issue of this journal, but has not been fully edited. Content may change prior to final publication. Citation information: DOI 10.1109/TIE.2022.3144590, IEEE Transactions on Industrial Electronics

semi-active topology, the SC is connected to the DC bus by a DC/DC converter whereas the battery is connected to the DC bus directly [30]. As a result, the supercapacitor is operated in a wide range of voltages with the help of the converter, whereas, the battery works passively to response the power requirement [31]. It should be noticed that the maximum capacity of a bidirectional DC/DC converter depends on the maximum power of the connected component. For the SC semi-active topology as shown in Fig. 1(a), it is the battery that connected to the DC bus via the DC/DC converter. Therefore, the DC/DC converter capacity is determined by the peak power of the battery. The battery, working as the high energy device, is protected by the SC from the very high power. Consequently, such topology releases the DC/DC converter from high power requirement. So, it is one of the potential advantages of the SC semi-active that it may be more cost- effective topology compared with the battery semi-active. Similar conclusions can also be found in the works [27, 28, 32]. However, in the SC semi-active scheme, the SC voltage is naturally clamped by the DC bus voltage, and the DC bus voltage is normally controlled as a constant, which lead to low utilization of SC capacitor [28].

Isolating the battery system from the instantaneous power fluctuation, meanwhile enabling the SC to operate within a highly effective range, the DC bus voltage on the SC semi-active method should be controlled in a deep range. However, the variable DC bus voltage will affect the devices mounted on the bus. Motor control in electric vehicles is a suitable application scenario for variable DC bus voltage control. Panda et al [33] presented a control strategy for the motor drive to reduce acoustic noise, where DC bus voltage is controlled as a function of speed. Jian et al [34] proposed a new HESS topology and variable DC bus voltage control strategy for electric drive vehicles, battery is isolated from frequent charges to increase the life of the battery. For the FFR, as an independent unit, the HESS has no interaction with other components on the DC bus. Therefore, in this study, a variable DC bus voltage control method is developed based on the SC semi-active hybrid topology, particularly for the FFR.

For HESS participating grid frequency modulation, there are critical requirements on the real-time performance of its power management algorithm [35]. For HESS, many algorithms can be found in the knowledge field. The rule-based strategy (RBS) is the most commonly used in practice, and in RBS power allocation among the different components is carried out according to the established rules [36]. Yin et al [37] propose a fuzzy logic control theory to distribute the power deviation according to the state of charge (SoC) of batteries and supercapacitors, this increases the battery life cycle due to the limited stress of the battery. Model predictive control (MPC) is another advanced method of HESS power allocation, which is used to control a process while satisfying a set of constraints. Recently, some methods based on machine learning or deep learning are developed to be used in the HESS power management dealing with the system nonlinearities. However, in terms of FFR application, there are some shortcomings in the above control strategy. For optimization approaches such as MPC, system state in serval future period needs to be predicted and calculated, which requires some calculation ability. A filter-based control strategy, which is able to take advantage of the inherent filtration characteristic of the SC so that to allocate low-frequency charge cycling to the battery, is more suitable for power allocation in HESS. The filter-based control strategy to allocate low-frequency charge cycling to the battery has been applied in HESS [38]. The efficiency of this control strategy is determined by the selection of the cut-off frequency. Asensio et al [39] presented a digital low-pass filter whose bandwidth is determined by the supercapacitor SoC. This algorithm could reduce frequent activation of controller protections while improving the energy utilization rate of supercapacitors. Wu et al [40] proposed good example that using artificial potential field-based dynamic filtering strategy for battery/SC HESS in electric vehicles. The artificial potential field strategy regulates the cutoff frequency of the power-split filter to reduces the charging and discharging current of the battery, and a feed-forward compensator is designed to compensate for load variations to counteract dc-link fluctuations. However, in the EV applications, the DC bus voltage need to maintained as a certain level with a fully active HESS topology, whereas in the frequency control a variable voltage control strategy may be more suitable. Therefore, this paper proposes a fuzzy-filter power management algorithm used for the variable voltage control within the HESS performing the FFR service. The contributions of this work are given as follows.

- Firstly, targeting at the newly published Firm frequency response in the UK, a hybrid energy storage system is designed and tested for the first time in the open literature to perform power system frequency regulation.
- Secondly, a variable voltage control within an SC semi-active hybrid scheme is developed and proven to be highly effective for the FFR service.
- Thirdly, power management integrating fuzzy logic with dynamic filtering is proposed benefits of broadening the filtering flexibility while reducing battery degradation.
- Finally, both the long-term simulations and short-term experiments are implemented to verify the feasibility of the proposed topology and control strategy.

This paper is organized as follows. Section II introduces the technical specification of the U.K Firm Frequency Response. The HESS topology and system modeling are introduced in Section III. Section IV illustrates the fuzzy-logic dynamic-filtering algorithm and variable voltage control strategy in detail. The long-term and short-term simulation results are analyzed in section V. Section VI shows the results of the scaled-down experiment, and the conclusions are presented in Section VII.

II. FFR Service: Technical Specification

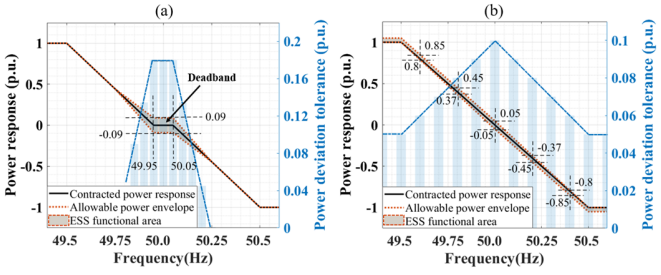

Fig. 2 (a) EFR functional envelope (b) FFR functional envelope

In order to maintain the grid frequency within the normal operating range ±1% of 50 Hz [13]. National Grid Electricity

This article has been accepted for publication in a future issue of this journal, but has not been fully edited. Content may change prior to final publication. Citation information: DOI 10.1109/TIE.2022.3144590, IEEE Transactions on Industrial Electronics

System Operator (ESO) has published two versions of frequency services with the enhanced frequency response (EFR) as shown in Fig. 2 (a) and the FFR as shown in Fig. 2 (b). The FFR is the new frequency service updated by 1st August 2019 [41]. Many previous works studied the ESSs used in the EFR, but there are only few works on the newly published FFR service. Compared with EFR, energy storage system in FFR need to deal with more short-term power fluctuations, which emphasize the higher requirements for the energy storage sectors.

As shown in Fig. 2, the maximum value of power response in EFR is 1.0 while that is 1.05 in FFR. For the same energy storage system, a larger range of power response means a higher charge/discharge rate. Another difference between the EFR and FFR is that the dead-band is clearly defined in the former whereas not in the latter. The energy storage system does not need to response in the dead-band. Therefore, for the battery system, it means frequent short-term charge/discharge processes in the FFR without dead-band, which will accelerate battery degradations. Also, the corresponding frequency to the power deviation tolerance is extended to a wider range in the FFR (49.5 to 50.5) compared with the EFR (49.75 to 50.25), which will result a higher power requirement for the same energy storage systems in the FFR case. With a supercapacitor in HESS, the battery will be protected from instantaneous high-power fluctuations. Therefore, compared with the EFR, the hybrid energy storage design may be more applicable in the FFR.

FFR services are divided into dynamic FFR (DFFR) and static FFR (SFFR). In the DFFR, the power demand/generation varies proportionally with the deviation of the system frequency, while the SFFR services are trigged at a pre-defined frequency deviation, and only a preset fixed power response is required within the operating period. The main features of the two types of service and differences between them are summarized as shown in Table I [5].

III. System Description

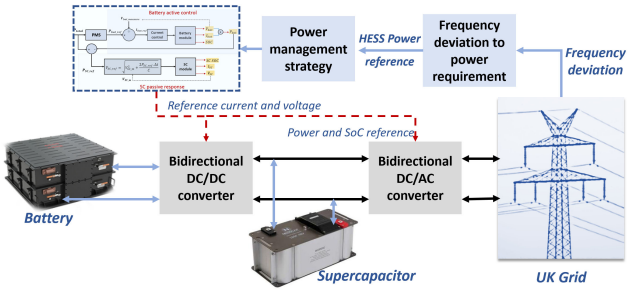

Fig. 3 Hybrid energy system configuration for the FFR

To mitigate the frequency fluctuations with the FFR envelope, the HESS unit connects to the main grid via the power converter as shown in Fig. 3. As discussed in the Introduction, the SC semi-active topology is particularly selected for the HESS used in the FFR. As shown in Fig. 3, the battery is connected to the DC bus through a DC/DC converter, while the SC connects to the DC bus directly, so its voltage varies with the DC bus voltage. For the traditional power control in the power grid, the DC bus voltage should be maintained as a certain value or around the constant value, which may lead to an extremely low SC utilization rate, and the SC only works as a normal filter in this case. Therefore, aiming to protect the battery from the instantaneous power fluctuations, meanwhile ensuring the SC is in a highly effective range, the DC bus voltage on the SC semi-active method should be controlled in a deep range. The variable bus voltage control strategy is therefore developed in this study, and introduced in detail in Section V.

The frequency deviations detected from the main grid are converted as the power requirements for the energy storage systems based on the FFR principle introduced in Section II, then, the energy management system illustrated in Section IV will share the power between the battery and the SC. The battery will be controlled by the DC/DC converter to track the power reference, whereas the SC compensates for the remaining power fluctuations. The supercapacitor model described in [42] is used in this study, and the equation of supercapacitor is described in Eq. 1.

$$V_{sc} = \frac{1}{C^*}\int\left((1+\frac{R_{esr}}{R_{leak}})I_{sc} - \frac{V_{sc}}{R_{leak}}\right)dt + I_{sc}R_{esr} \tag{1}$$

R_{leak} is the leakage resistance, R_{esr} is the series resistance, and C^* is the effective capacitance of SC. It should be noted that compare with the leakage resistance, the series resistance is relatively small, so the Eq. (1) can be approximately written as Eq. (2).

$$V_{sc} = \frac{1}{C^*}\int\left(I_{sc} - \frac{V_{sc}}{R_{leak}}\right)dt + I_{sc}R_{esr} \tag{2}$$

The state of charge (SoC) of the battery is defined to describe the ratio between the current charges over the capacity, and the battery capacity model can be described as shown in Eq. (3).

$$SoC(t+1) = \begin{cases} SoC(k) - \eta_C \dfrac{T_S}{Q} I_{Batt}(k): I_{Batt}(k) \le 0 \\ Soc(k) - \dfrac{T_S}{\eta_D Q} I_{Batt}(k): I_{Batt}(k) \ge 0 \end{cases} \tag{3}$$

where T_s is the sampling time, η_c and η_D define the charge/discharge efficiency of the battery. I_{Batt} represent the battery charge/discharge, the positive value implies that the battery supplies energy while the negative sign implies the battery absorbs energy.

TABLE I. Characteristics Comparison of SFFR and DFFR [5]

FFR product type	Service target	Service type	Service speed	Length of response
SFFR (Static Firm Frequency Response)	Secondary response only	SFFR is triggered at a defined frequency deviation which must be in place befotablere tendering.	⩽30 secs	30 mins
DFFR (Dynamic Firm Frequency Response)	Primary, High, and Secondary response	DFFR is used to manage frequency variations within the second by second operating range	Primary: ⩽2 secs	20 secs
			High: ⩽10 secs	Indefinitely unless otherwise agreed
			Secondary: ⩽30 secs	30 mins

This article has been accepted for publication in a future issue of this journal, but has not been fully edited. Content may change prior to final publication. Citation information: DOI 10.1109/TIE.2022.3144590, IEEE Transactions on Industrial Electronics

IV. Power Management and Control

A. An improved dynamic power filtering algorithm

The low-pass filtering algorithm is one of the most commonly used power allocation algorithms for the hybrid energy storage system. Compare with others, the control process of the filtering algorithm is very straightforward which could ensure the real-time performance of the hybrid system, so it is widely used in practical engineering applications. In the HESS, the power reference is divided into high-frequency components responded by supercapacitor and low-frequency components responded by the battery. However, the key problem for the power filtering algorithm is that the cut-off frequency of the filtering is constant and set empirically based on the applications. That may limit the optimal operation of the energy storage system. For example, in the FFR, the sensitivity and smoothness of battery power reference (BPR) cannot be satisfied at the same time because of the constant cut-off frequency. Therefore, the dynamic filtering algorithm which is able to adjust the cut-off frequency dynamically according to the real-time power conditions is proposed and used in many studies [40]. However, the cut-off frequency is changed referencing the power conditional in the next control step, which may result in a slight delay in the control loop. However, the power system frequency is varying second by second calling for a real-time control capability for the energy storage systems.

This paper proposes a fuzzy-logic dynamic-filtering (FLDF) algorithm to balance the sensitivity and smoothness, meanwhile, maintaining the real-time control capability of the power. Energy management strategy based on filter could take advantage of high power-density characteristic of supercapacitor. In FLDF algorithm, the battery is prevented from violent charging and discharging. By formulating appropriate fuzzy rules to adjust the filter parameters, the balance between sensitivity and smoothness can be achieved. The improved dynamic power filtering algorithm is divided into two parts: filter parameters calculation based on fuzzy logic (FL) and dynamic filtering power allocation.

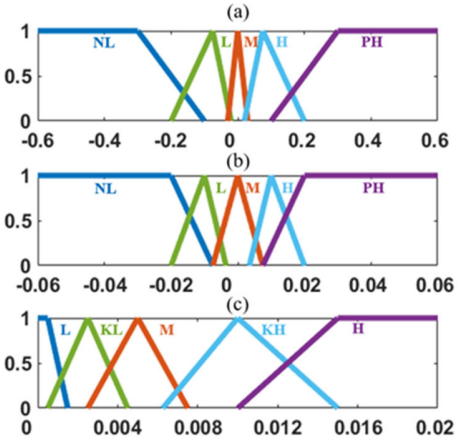

Fig. 4 (a) Power demand fuzzification (b) Power demand deviation fuzzification (c) filter parameter defuzzification

As a typical fuzzy logic design, the fuzzy logic controller of the HESS has two inputs which are HESS power demand (P) and power demand variation (dP), and the output is filter parameters (K_f). Fig. 4 is used to clarify the "fuzzification" and "defuzzification" processes. The input variable HESS power demand P has five fuzzy values including negative low (NL), low (L), medium (M), high (H), and positive high (PH). Fig. 4(a) and (b) illustrate the power demand fuzzification and power demand deviation fuzzification, respectively. In the proposed power system, for example, when P is positive, the power flow direction is from HESS to the grid. The value of dP is the difference between the power at the present and that at the previous moment. Similarly, the input variable dP also has five fuzzy values. The output value K_f is the filter parameter of the dynamic filtering algorithm. As shown in Fig.4 (c), it has five fuzzy values. Both KL and KH are the part of the K_f fuzzy value. KL is the fuzzy value between low (L) and medium (M), and KH is the fuzzy value between medium (M) and high (H). When K_f is at a higher value, the sensitivity of battery power reference increases, power reference decreases. By formulating appropriate fuzzy rules, the balance between sensitivity and smoothness can be achieved.

TABLE II Fuzzy Logic Rules of FLDF

		dP				
		PH	H	M	L	NL
P	PH	KL	L	L	KH	H
	H	H	KH	M	KH	H
	M	H	KH	H	KH	H
	L	H	KH	M	KH	H
	NL	H	KH	L	L	KL

The correspondence between input and output variables is listed in Table II. K_f will be set at max value with the medium HESS power demand. When the power is in high state, a lower value will be set to K_f to ensure the smoothness of the battery power reference in the condition where dP is high or positive high. The higher the reference of HESS power, the faster the variation of power variation is, and the lower the value of the filter parameter will be. The surface of the proposed fuzzy logic control is shown in Fig. 5(a). It is obvious that K_f is set to the high level when HESS power demand and its variation are both at the medium level, and in this case, the majority part of power demand is provided by the battery. The relationship between filter parameters and power allocation is shown in Fig. 5(b). The higher the value of K_f is, the greater the power the battery will respond.

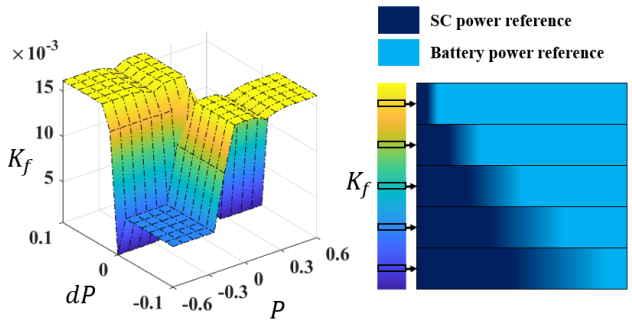

(a) (b)

Fig. 5 (a) The control surface of the fuzzy logic control (b) The relationship between filter parameters and power allocation

Through fuzzy logic control, this filtering algorithm could balance the sensitivity and smoothness of battery power reference in this study to prevent violent charging and discharging of the battery in various power cases.

This article has been accepted for publication in a future issue of this journal, but has not been fully edited. Content may change prior to final publication. Citation information: DOI 10.1109/TIE.2022.3144590, IEEE Transactions on Industrial Electronics

B. *Variable voltage control strategy*

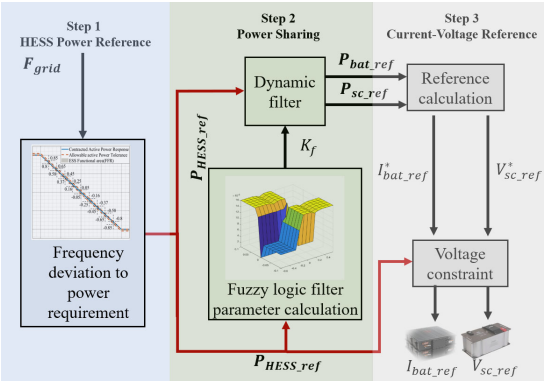

Fig. 6 The proposed variable voltage control

To keep the battery from direct impact of the power requirement, at the same time to explore a deep range of the SC functional area, new variable voltage control is developed particularly for HESS used in the FFR services. The variable voltage here means the variable DC bus voltage is the same as the SC voltage, and it should be set with an appropriate range. The upper limit V_{max} cannot be higher than the SC rated voltage, so it is set as 95% of the rated voltage as to improve the usage of supercapacitor. Since the synchronous rectifier buck DC/DC converter is used in this study, the DC bus voltage cannot be lower than battery voltage as to guarantee correct switch modes. Therefore, the lower limit V_{min} is set as battery rated voltage to improve the SC utilization as much as possible. The utilization of SC in the proposed semi-active topology could reach 70.5%. As shown in Fig. 6, the proposed control strategy can be divided into three steps.

Step 1: HESS power reference.

Based on the FFR converting principle, as illustrated in Section II, the FFR block is used to convert the frequency signal into a power signal while ensuring that the output power meets the FFR constraint. In this step, the power requirement from the HESS for the FFR is obtained as the HESS power reference, P_{HESS_ref}.

Step 2: Power sharing.

Based on the proposed fuzzy-logic dynamic-filtering algorithm, the optimal power for each energy storage system is allocated in this step. The cut-off frequency K_f will adaptively change based on the real-time condition of the HESS power reference and will return to a trade-off between the sensitivity and smoothness for the battery power control. In the meantime, the SC will compensate for the remaining power fluctuations.

Step 3: Current and voltage reference

The power reference will be translated to the DC bus voltage reference (same with the SC voltage) and battery current control references $I^*_{bat\_ref}$ in this step. Battery current reference is determined by Eq.3, where the V_{bat} is the measurement of battery system terminal voltage. P_{bat_ref} is the power reference of the battery allocated by the FLDF algorithm.

$$I^*_{bat\_ref} = \frac{P_{ref}}{V_{bat}} \tag{4}$$

The energy stored by the supercapacitor (E_{SC}) is determined by supercapacitor voltage (V_{SC}) and capacity (C) (Eq.4). When the control time-step Δt is selected, the DC bus voltage reference $(V^*_{SC\_ref})$ could be calculated by Eq.5, where P_{SC_ref} is the power reference of supercapacitor.

$$E_{sc} = \frac{1}{2}CV_{sc}^2 \tag{5}$$

$$V^*_{sc\_ref} = \sqrt{\frac{2P_{sc\_ref}\Delta t}{C} + V_{sc}^2\ (t-1)} \tag{6}$$

The voltage constraint block as shown in Fig. 6 is used to prevent the DC bus voltage from buckling failure. With this block, supercapacitor voltage can only fluctuate within a preset range. The value of V_{max} is 95% of the rated SC voltage to maximize the use of supercapacitor. The DC bus voltage cannot be set lower than battery voltage as to guarantee correct switch mode of the DC/DC converter. Therefore, the Vmin is set as battery rated voltage. The utilization of SC in this design reaches 70.5%. Besides, the SoC works as the constraints for the control algorithm. For example, for the battery with SoC$\in$ [0.2, 0.85], is set as the upper and lower limit. Therefore, based on the HESS power reference the battery power reference could be reset to ensure HESS power response meets the FFR constraint.

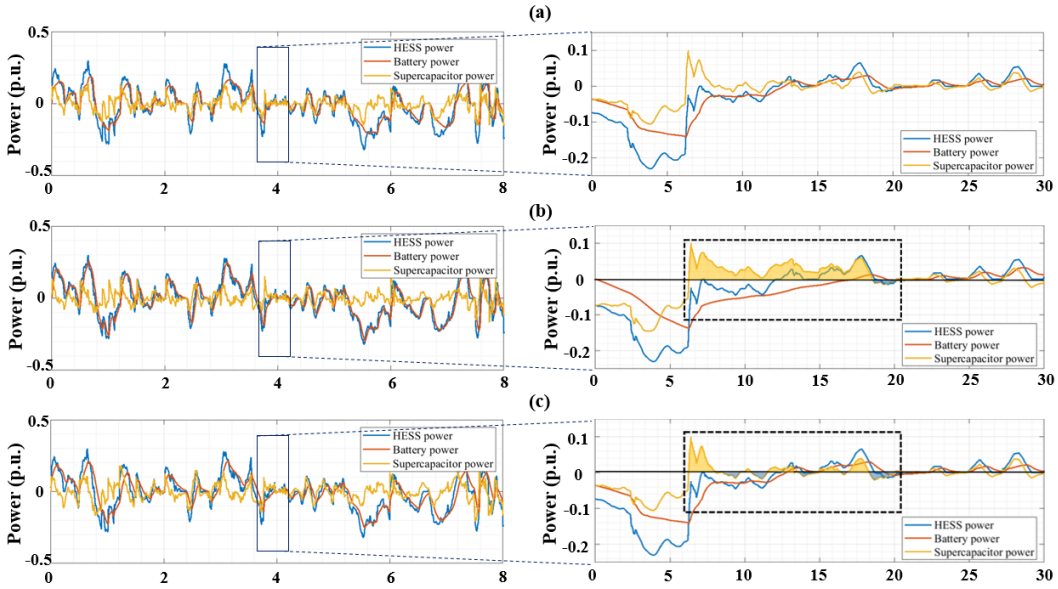

Fig. 7 Comparison of power distributions in three cases with 8-hours power window and 30-mins power window (a). constant filtering case; (b). traditional dynamic filtering case (c) FLDF case

This article has been accepted for publication in a future issue of this journal, but has not been fully edited. Content may change prior to final publication. Citation information: DOI 10.1109/TIE.2022.3144590, IEEE Transactions on Industrial Electronics

V. Simulation Results

TABLE III. Parameters of Major Components of the Simulation

Battery rated voltage	607 V
Battery rated capacity	0.7MWh
Supercapacitor rated voltage	1366V
Supercapacitor rated capacity	0.07MWh
Maximum DC bus voltage	1300V
Minimum DC bus voltage	607V
DC/DC converter rated power capability	1MVA

Firstly, in this study, simulation work is designed to verify the FLDF algorithm. Constant filtering algorithms and dynamic filter algorithms are used as comparisons. The Willenhall Energy Storage System (WESS) [13] in the UK is used as the reference in the proposed simulation. However, the WESS is a battery-only-system, so we made some modifications on the HESS. The battery is set as 0.7 MWh and that is 0.07 MWh for the supercapacitor. The detailed parameters can be found in Table III. The frequency signal is downloaded from the historic frequency data of NG, with the eight hours frequency fluctuations (12:00- 20:00 7th Sep 2020) as the input for the frequency to power converting. Then, the eight hours power requirement for the HESS in the FFR is used as the same case for the three power management algorithms.

Fig. 7 shows the simulation results comparison of different power allocation strategies. It is obvious that a relatively large cut-off frequency is selected for the low-pass filtering algorithm as shown in Fig. 7(a), which results in the over-sensitivity of the battery for the power changes. Therefore, as shown in the 8-hours power window, the battery power (red curve) almost coincides with the blue curve that the total power requirement. In these cases, the SC is not fully used to respond to the high frequency power fluctuations. This may also lead to a deeper charge/discharge of the battery as shown in the 30-mins power windows as shown in Fig. 7 (a). Variable filtering parameter is set to a larger value automatically when the energy storage systems suffer from a serious power change, and vice versa as shown in Fig. 7 (b). The dynamic changes of the cut-off frequency are determined by the "next-second" power conditions with the delays, which may lead to the performance, as shown in Fig. 7 (b) that the battery is insensitive to the power changes. With the proposed FLDF algorithm, however, the filtering parameters changed with power and power deviations. As shown in the Fig. 7 (b) and (c), the highlighted orange part represents the SC discharged energy, and the highlighted blue part represents the SC charged energy. It is obvious that the discharged energy of the SC in case (b) is more than that in case (c). This shows the advantages of the FLDF that it will return a better trade-off between sensitivity and smoothness according to the power and power deviation. Size setting of SC in case (b) and (c) are the same, and the different filtering parameters lead to the different performance of the SC in (b) and (c). As shown in Fig. 7 (c), battery power curve coincides with total power curve basically when the total power fluctuates slightly, and SC will respond to sudden power change.

Secondly, the state of charge is an important parameter for the battery energy storage, and it is one of the key factors that could be used to evaluate the battery degradation process. The SoC of the battery is used to evaluate and test the different control strategy, as shown in Fig. 8. based on the same topology (SC semi-active) the variable voltage control method is also compared with the constant voltage control as shown in Fig. 8. It is very obvious that variable voltage control has a very high SC utilization rate as exploring a deeper range of the DC bus voltage. As a result, compare with Fig.8(e) and 8(f), the battery is controlled more smoothly and has a much better functional area as shown in Fig. 8(b) and 8(c).

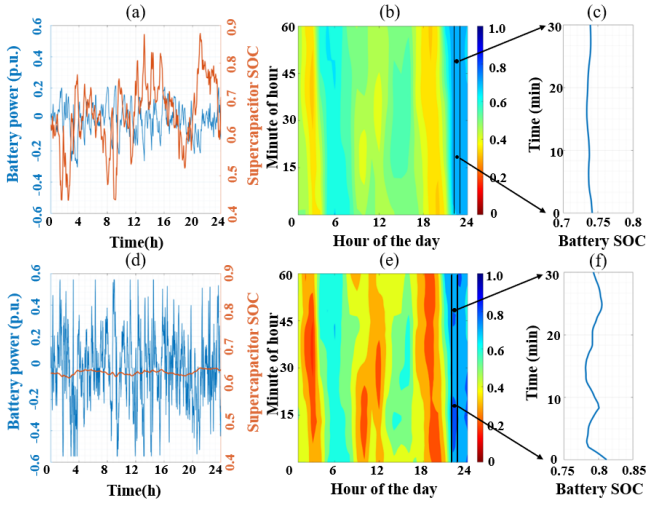

Fig. 8 Comparison of the battery power, battery SoC and supercapacitor SoC in VVC case(a-c) and CVC case (d-f)

To further verify the effectiveness of the fuzzy logic dynamic filtering algorithm with the variable voltage control strategy, a series of case studies are carried out and compared accordingly in this paper.

A week of frequency data of the British grid in the first week of December 2018 is used in the case studies. The five cases shown in Table IV are made based on different topologies and control methods. For example, case 1 as a benchmark case, is made based on the fully active topology. Case 2 is the proposed SC-semi active topology and VVC strategy.

TABLE IV
The Combination of Different Topology and Control Strategy

Case	Topology	Control strategy
1	Fully Active	FLDF with CVC strategy
2	SC semi-active	FLDF with VVC strategy
3	Battery semi-active	FLDF with CVC strategy
4	SC semi-active	FLDF with CVC strategy
5	Battery only system	PID control with CVC

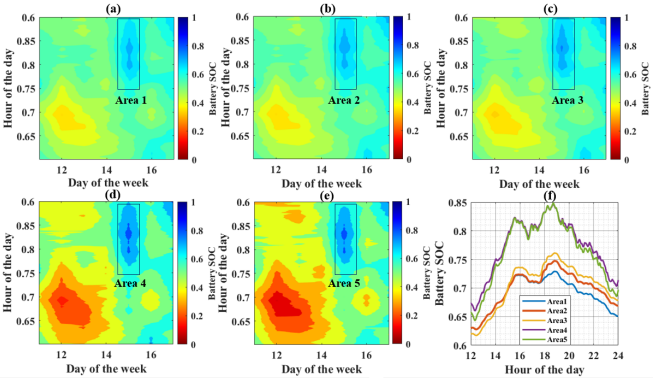

Fig. 9. (a) Battery SoC obtained by the case1 (b) Battery SoC obtained by the case2 (c) Battery SoC obtained by the case3 (d) Battery SoC obtained by the case4 (e) Battery SoC obtained by the case5 (f)SoC comparison between different cases

The battery SoC profiles in the selected 7 days are shown and compared in Fig. 9. It is very obvious that the battery in case 1

This article has been accepted for publication in a future issue of this journal, but has not been fully edited. Content may change prior to final publication. Citation information: DOI 10.1109/TIE.2022.3144590, IEEE Transactions on Industrial Electronics

has the best performance as both the SC and battery are fully controlled in this case. Case 2 (Fig. 9(b)) and case 3 (Fig. 9(c)) have similar preferences. The only difference is that the battery has a slightly deeper SoC range in case 3 than that in case 2. However, the power rate of the DC/DC power converter in case 3 should be larger than that in case 2, as in the battery semi-active topology, the SC dealing with the high power connected to the DC bus via the converter. The battery system in case 5 has widely SoC variation range and severe SoC fluctuation as all the power requirements for the FFR need to be dealt with by the battery. HESS with the SC semi-active topology and constant voltage control (case 4) is similar to a battery-only system since the SC, in this case, does not make any contributions to mitigate the power fluctuations.

The battery life degradation is also estimated based on the rain-flow cycle-counting algorithm. The rain-flow counting method is used to statistics cover the number and the depth of discharge of each charging-discharging cycle and half cycles based on SoC curve [43]. Then, the battery life degradation of each cycle could be obtained referring the cycle to failure (CTF) curve. Consequently, the total battery life degradation is the summary of each cycle degradation. It should be noticed that in this study, only the battery SoC (depth of discharge) is used in the evaluation, whereas other factors such as the discharging rate and temperature are not considered within the battery lifetime model. A detailed introduction about this battery lifetime model can be found in [44]. The results for the five cases are shown in Table V, which indicates that the proposed HESS is working as expected, and by using the variable voltage control strategy, the control effect achieved by the semi-active topology is close to the fully active topology. Since only one DC/DC converter is required, the cost of semi-active topology is lower than that of active topology. Therefore, in scenarios where variable voltage can be applied, semi-active topology is a suitable choice for hybrid energy storage system.

TABLE V
BATTERY AGE CALCULATION USING RAIN FLOW ALGORITHM

Case	Case 1	Case 2	Case 3	Case 4	Case 5
Battery degradation	0.326%	0.336%	0.343%	0.409%	0.417%

VI. EXPERIMENTAL VERIFICATION

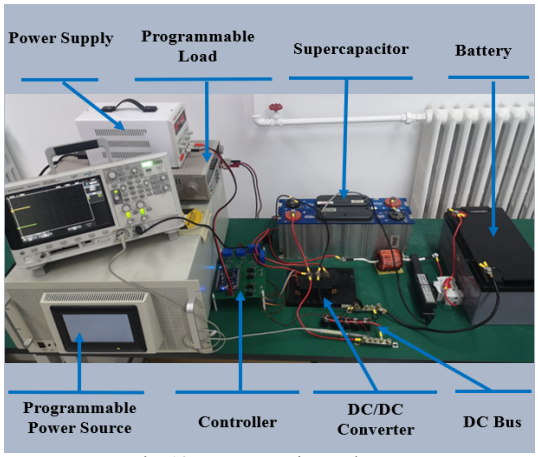

Fig. 10 HESS experimental setup

A scaled-down HESS experiment platform (shown in Fig. 10) is set up to verify the feasibility and real-time performance of the proposed VVC with the SC semi-active topology for the FFR. The parameters of the components used in the experiment are listed in Table VI. Among these components, the controller and DC/DC converter is designed and manufactured in-house.

TABLE VI
PARAMETERS OF MAJOR COMPONENTS OF THE EXPERIMENTAL SETUP

Battery	12V 65AH (LC-P1265)
Supercapacitor	27.0V 10.0F (SZFXSC)
DC/DC converter	Synchronous rectifier buck DC/DC converter including Intelligent Power Modules (IPM400DV1A060) and 500uH inductance, operating at frequencies to 20kHz.
Controller	TMS320F28335

The power demand data used in the experiment is converted from the frequency data of 18:00-20:00 on September 11, 2020. Since variable load is programmed to provide negative power only, in this experiment, the power demand of HESS is implemented by using a programmable power source and programmable load. A variable bus control strategy with FLDF power-sharing method is implemented in the TMS320F28335 controller. The SC is connected directly to the DC bus while the battery by a DC/DC converter, forming the SC semi-active topology. Constant DC bus voltage control with the same topology is set as the control group. The DC range of the DC bus voltage is scaled as 12 V to 20 V.

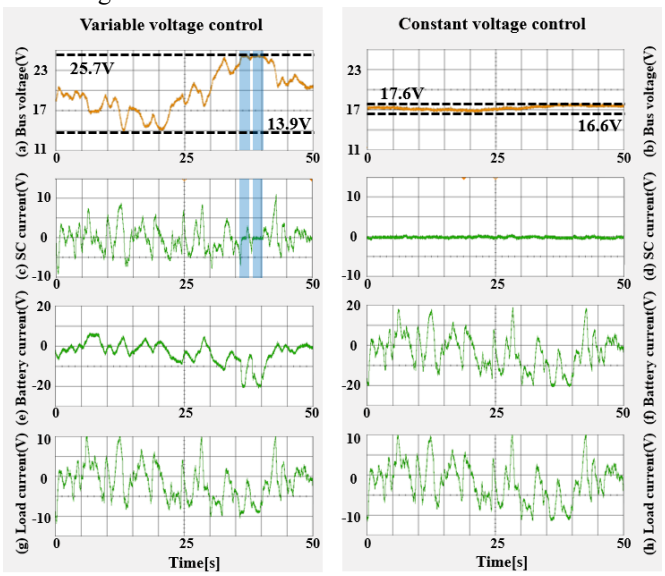

Fig. 11 Experiment results

The Fig. 11 gives the comparisons between the proposed variable voltage control and the constant voltage control. It is obvious that the SC voltage range is much wider with the variable voltage control than that in the constant voltage control. This leads to the different usage rate of the SC in the two control methods. As shown in the Fig. 11 (a), in the variable voltage control, the SC voltage fluctuates from 13.9 V to 25.7 V, while SC voltage in constant varies in a very narrow range (16.6V - 17.6V), as shown in Fig. 11 (b). As a result, the SC will have a very narrow functional area with utilization rate of 4.6%, whereas the battery needs to response to frequent and serve power changes as shown in Fig. 11 (d) and (f). In contrast, with the variable voltage control, the battery has much smoother power contributions as shown in Fig. 11 (e), as the SC works at a large voltage range. In this case, the supercapacitor utilization is 64.1%. Furthermore, the saturation cases of the supercapacitor are tested in the experiments as highlighted in blue area shown in Fig. 11 (a) and (c). It should be figured out

that, the up-limit of the DC bus is set as 95% of the rated SC voltage as to improve the usage of supercapacitor. It is obvious that continuous charging will saturate the SC, making it reach the DC bus up-limit as highlighted in Fig. 11 (a). During this period, the SC current will maintain at zero, and the battery deals with the entire load power. It should be noted that the same SC is used in the two different experiment, and only the control strategies are different in these two cases.

Acknowledgement

This work was supported by the Nature Science Foundation of China with Grant No. 52172354 and Jianwei Li would like thank the supported by China Association for Science and Technology Youth Talent Promotion Project.

VII. Conclusion

Compared with enhanced frequency response, firm frequency response has no dead-band but with a wider frequency response range. Therefore, energy storage system in FFR need to deal with more short-term power fluctuations, which emphasize the higher requirements for the energy storage sectors. This paper proposes a hybrid energy storage shame with a variable voltage control based on a SC semi-active topology benefiting in improving the SC utilization rate meanwhile reducing battery degradation. A fuzzy logic based dynamic filtering algorithm is designed for this topology to realize the power distribution between the supercapacitor and battery. Quantitative comparisons of battery degradations and SC use ratios are used to test the suggested topology with the control method and power management, in both long-term simulations and scaled-down experiments. In this study, the variable bus voltage control strategy is proved to be an effective method for the hybrid energy storage system to participate UK grid frequency regulation. In the FFR, HESS works as a stand-alone component so that the variable DC bus voltage is applicable. Therefore, the proposed methods can be potentially used in other applications in which the hybrid energy storage has no interaction with other parallel components on the DC bus.

References

[1] D. Greenwood, K. Y. Lim, C. Patsios, P. Lyons, Y. S. Lim, and P. Taylor, "Frequency response services designed for energy storage," *Applied Energy,* vol. 203, pp. 115-127, 2017.

[2] L. Fu, J. Zhang, S. Xiong, Z. He, and R. Mai, "A modified dynamic synchrophasor estimation algorithm considering frequency deviation," *IEEE Transactions on smart grid,* vol. 8, no. 2, pp. 640-650, 2016.

[3] C. A. Agostini, F. A. Armijo, C. Silva, and S. Nasirov, "The role of frequency regulation remuneration schemes in an energy matrix with high penetration of renewable energy," *Renewable Energy,* vol. 171, pp. 1097-1114, 2021.

[4] B. Jie, T. Tsuji, and K. Uchida, "Analysis and modelling regarding frequency regulation of power systems and power supply–demand-control based on penetration of renewable energy sources," *The Journal of Engineering,* vol. 2017, no. 13, pp. 1824-1828, 2017.

[5] N. G. ESO. *Firm Frequency Response (FFR) Interactive Guidance*. Available: https://www.nationalgrid.com/sites/default/files/documents/Firm%20Frequency%20Response%20%28FFR%29%20Interactive%20Guidance%20v1%200_0.pdf

[6] A. Postnikov, I. Albayati, S. Pearson, C. Bingham, R. Bickerton, and A. Zolotas, "Facilitating static firm frequency response with aggregated networks of commercial food refrigeration systems," *Applied Energy,* vol. 251, p. 113357, 2019.

[7] B. M. Gundogdu, S. Nejad, D. T. Gladwin, M. P. Foster, and D. A. Stone, "A battery energy management strategy for UK enhanced frequency response and triad avoidance," *IEEE Transactions on Industrial Electronics,* vol. 65, no. 12, pp. 9509-9517, 2018.

[8] H. Zhao, M. Hong, W. Lin, and K. A. Loparo, "Voltage and frequency regulation of microgrid with battery energy storage systems," *IEEE Transactions on smart grid,* vol. 10, no. 1, pp. 414-424, 2017.

[9] M. Datta and T. Senjyu, "Fuzzy control of distributed PV inverters/energy storage systems/electric vehicles for frequency regulation in a large power system," *IEEE Transactions on Smart Grid,* vol. 4, no. 1, pp. 479-488, 2013.

[10] Q. Shi, F. Li, Q. Hu, and Z. Wang, "Dynamic demand control for system frequency regulation: Concept review, algorithm comparison, and future vision," *Electric Power Systems Research,* vol. 154, pp. 75-87, 2018.

[11] K. S. El-Bidairi, H. D. Nguyen, T. S. Mahmoud, S. Jayasinghe, and J. M. Guerrero, "Optimal sizing of Battery Energy Storage Systems for dynamic frequency control in an islanded microgrid: A case study of Flinders Island, Australia," *Energy,* vol. 195, p. 117059, 2020.

[12] L. Barelli, G. Bidini, and F. Bonucci, "A micro-grid operation analysis for cost-effective battery energy storage and RES plants integration," *Energy,* vol. 113, pp. 831-844, 2016.

[13] B. Gundogdu, D. Gladwin, and D. Stone, "Battery energy management strategies for UK firm frequency response services and energy arbitrage," *The Journal of Engineering,* vol. 2019, no. 17, pp. 4152-4157, 2019.

[14] B. Xu, A. Oudalov, J. Poland, A. Ulbig, and G. Andersson, "BESS control strategies for participating in grid frequency regulation," *IFAC Proceedings Volumes,* vol. 47, no. 3, pp. 4024-4029, 2014.

[15] J. Li, R. Xiong, Q. Yang, F. Liang, M. Zhang, and W. Yuan, "Design/test of a hybrid energy storage system for primary frequency control using a dynamic droop method in an isolated microgrid power system," *Applied Energy,* vol. 201, pp. 257-269, 2017.

[16] M. Świerczyński, D. I. Stroe, A. I. Stan, and R. Teodorescu, "Primary frequency regulation with Li-ion battery energy storage system: A case study for Denmark," pp. 487-492: IEEE.

[17] G. Li, Z. Yang, B. Li, and H. Bi, "Power allocation smoothing strategy for hybrid energy storage system based on Markov decision process," *Applied Energy,* vol. 241, pp. 152-163, 2019.

[18] W. Jing, C. H. Lai, W. S. Wong, and M. D. Wong, "Dynamic power allocation of battery-supercapacitor hybrid energy storage for standalone PV microgrid applications," *Sustainable Energy Technologies,* vol. 22, pp. 55-64, 2017.

[19] J. Li, M. Zhang, Q. Yang, Z. Zhang, and W. Yuan, "SMES/battery hybrid energy storage system for electric buses," *IEEE Transactions on Applied Superconductivity,* vol. 26, no. 4, pp. 1-5, 2016.

[20] Z. Zheng, X. Wang, and Y. Li, "A control method for grid-friendly photovoltaic systems with hybrid energy storage units," in *2011 4th International Conference on Electric Utility Deregulation and Restructuring and Power Technologies (DRPT)*, 2011, pp. 1437-1440: IEEE.

[21] N. R. Tummuru, M. K. Mishra, and S. Srinivas, "Dynamic energy management of renewable grid integrated hybrid energy storage system," *IEEE Transactions on Industrial Electronics,* vol. 62, no. 12, pp. 7728-7737, 2015.

[22] J. Li, Q. Yang, F. Robinson, F. Liang, M. Zhang, and W. Yuan, "Design and test of a new droop control algorithm for a SMES/battery hybrid energy storage system," *Energy,* vol. 118, pp. 1110-1122, 2017.

[23] X. Chen, J. Zhou, M. Shi, L. Yan, W. Zuo, and J. Wen, "A Novel Virtual Resistor and Capacitor Droop Control for HESS in Medium-Voltage DC System," *IEEE Transactions on Power Systems,* vol. 34, no. 4, pp. 2518-2527, 2019.

[24] J. Li *et al.*, "Analysis of a new design of the hybrid energy storage system used in the residential m-CHP systems," *Applied Energy,* vol. 187, pp. 169-179, 2017.

[25] J. C. Hernandez, P. G. Bueno, and F. Sanchez-Sutil, "Enhanced utility-scale photovoltaic units with frequency support functions and dynamic grid support for transmission systems," *IET Renewable Power Generation,* vol. 11, no. 3, pp. 361-372, 2017.

[26] M. Rezkalla, A. Zecchino, S. Martinenas, A. M. Prostejovsky, and M. Marinelli, "Comparison between synthetic inertia and fast frequency containment control based on single phase EVs in a microgrid," *Applied Energy,* vol. 210, pp. 764-775, 2018.

[27] H. Chen, Z. Zhang, C. Guan, and H. Gao, "Optimization of sizing and frequency control in battery/supercapacitor hybrid energy storage system for fuel cell ship," *Energy,* p. 117285, 2020.

This article has been accepted for publication in a future issue of this journal, but has not been fully edited. Content may change prior to final publication. Citation information: DOI 10.1109/TIE.2022.3144590, IEEE Transactions on Industrial Electronics

[28] Z. Song, H. Hofmann, J. Li, X. Han, X. Zhang, and M. Ouyang, "A comparison study of different semi-active hybrid energy storage system topologies for electric vehicles," *Journal of Power Sources,* vol. 274, pp. 400-411, 2015.

[29] S. Barcellona, L. Piegari, and A. Villa, "Passive hybrid energy storage system for electric vehicles at very low temperatures," *Journal of Energy Storage,* vol. 25, p. 100833, 2019.

[30] Z. Song *et al.*, "Multi-objective optimization of a semi-active battery/supercapacitor energy storage system for electric vehicles," *Applied Energy,* vol. 135, pp. 212-224, 2014.

[31] M. Ortúzar, J. Moreno, and J. Dixon, "Ultracapacitor-based auxiliary energy system for an electric vehicle: Implementation and evaluation," *IEEE Transactions on industrial electronics,* vol. 54, no. 4, pp. 2147-2156, 2007.

[32] F. Ju, Q. Zhang, W. Deng, and J. Li, "Review of structures and control of battery-supercapacitor hybrid energy storage system for electric vehicles," in *2014 IEEE International Conference on Automation Science and Engineering (CASE)*, 2014, pp. 143-148: IEEE.

[33] D. Panda and V. Ramanarayanan, "Reduced acoustic noise variable DC-bus-voltage-based sensorless switched reluctance motor drive for HVAC applications," *IEEE Transactions on Industrial Electronics,* vol. 54, no. 4, pp. 2065-2078, 2007.

[34] C. Jian and A. Emadi, "A New Battery/UltraCapacitor Hybrid Energy Storage System for Electric, Hybrid, and Plug-In Hybrid Electric Vehicles," *IEEE Transactions on Power Electronics,* vol. 27, no. 1, pp. 122-132, 2012.

[35] Q. Yang *et al.*, "An improved vehicle to the grid method with battery longevity management in a microgrid application," *Energy,* vol. 198, p. 117374, 2020.

[36] A. Geetha and C. Subramani, "A comprehensive review on energy management strategies of hybrid energy storage system for electric vehicles," *International Journal of Energy Research,* vol. 41, no. 13, pp. 1817-1834, 2017.

[37] H. Yin, W. Zhou, M. Li, C. Ma, and C. Zhao, "An adaptive fuzzy logic-based energy management strategy on battery/ultracapacitor hybrid electric vehicles," *IEEE Transactions on transportation electrification,* vol. 2, no. 3, pp. 300-311, 2016.

[38] D. B. W. Abeywardana, B. Hredzak, V. G. Agelidis, and G. D. Demetriades, "Supercapacitor sizing method for energy-controlled filter-based hybrid energy storage systems," *IEEE Transactions on Power Electronics,* vol. 32, no. 2, pp. 1626-1637, 2016.

[39] E. M. Asensio, G. A. Magallán, C. H. De Angelo, and F. M. Serra, "Energy management on battery/ultracapacitor hybrid energy storage system based on adjustable bandwidth filter and sliding-mode control," *Journal of Energy Storage,* vol. 30, p. 101569, 2020.

[40] Y. Wu *et al.*, "Adaptive power allocation using artificial potential field with compensator for hybrid energy storage systems in electric vehicles," *Applied Energy,* vol. 257, p. 113983, 2020.

[41] N. G. ESO. *FFR Dynamic FFR Analysis Tool User Guide 2019*. Available: https://www.nationalgrideso.com/document/148821/download

[42] A. M. Gee, F. V. Robinson, and R. W. Dunn, "Analysis of battery lifetime extension in a small-scale wind-energy system using supercapacitors," *IEEE transactions on energy conversion,* vol. 28, no. 1, pp. 24-33, 2013.

[43] H. Wang, H. He, Z. Wei, Q. Yang, and P. Igic, "Battery Optimal Sizing under a Synergistic Framework with DQN Based Power Managements for the Fuel Cell Hybrid Powertrain," *IEEE Transactions on Transportation Electrification,* 2021.

[44] J. Li, A. M. Gee, M. Zhang, and W. Yuan, "Analysis of battery lifetime extension in a SMES-battery hybrid energy storage system using a novel battery lifetime model," *Energy,* vol. 86, pp. 175-185, 2015.

Jianwei Li (M'17) received the B.Eng. degree from North China Electric Power University and the Ph.D. degree in Electrical Engineering from the University of Bath, U.K. He has worked with the University of Liege, Beijing Institute of Technology, CU and University of Oxford. His research interests include electrical energy storages and hybrid energy storages, electrical vehicles, batteries, fuel cells, hydrogen energy, hydrogen energy safty and power management of the multi-vector system.

Fang Yao was born in Wuhu, Anhui, China in 1998. He received the B.S. degree in Electrical Engineering and Automation from Beijing Institute of Technology. He is currently pursuing the M.S. degree in vehicle engineering at Beijing Institute of Technology. His research interests include power management strategy for the hybrid energy storage system and grid frequency modulation.

Qingqing Yang (S'14, M'17) received Ph.D. degree from the University of Bath, U.K. She worked as a Lead Engineer on the electrical engineering in the Beijing Electric Power Research Institute, State Grid Corporation of China. She is currently a Lecture with Coventry University. Her research interests include applied superconductivity, virtual inertia in the power systems and artificial intelligence applications in energy storage and smart grids.

Zhongbao Wei (M'19) received the B.Eng. and the M.Sc. degrees in instrumental science and technology from Beihang University, China, in 2010 and 2013, and the Ph.D. degree in power engineering from Nanyang Technological University, Singapore, in 2017. He is currently a Professor with School of Mechanical Engineering, Beijing Institute of Technology, China. His research interests include modeling, identification, state estimation, diagnostic for battery system, and energy management for hybrid energy systems.

Hongwen He (M'03–SM'12) received the M.Sc. degree from the Jilin University of Technology, Changchun, China, in 2000 and the Ph.D. degree from the Beijing Institute of Technology, Beijing, China, in 2003, both in vehicle engineering. He is currently a Professor with the National Engineering Laboratory for Electric Vehicles, Beijing Institute of Technology. His research interests include power battery modeling and simulation on electric vehicles, design, and control theory of the hybrid power trains.